FED-Vol. 210, Cavitation and Multiphase Flow
ASME 1995

BUBBLE DYNAMICS EFFECTS ON THE ROTORDYNAMIC FORCES IN CAVITATING INDUCERS

Fabrizio d'Auria, Luca d'Agostino
Dipartimento di Ingegneria Aerospaziale
Università degli Studi di Pisa
Pisa, Italy

Christopher E. Brennen
California Institute of Technology
Pasadena, California

ABSTRACT

The present work investigates the dynamics of idealized bubbly and cavitating flows in whirling helical inducers, with the purpose of understanding the impact of the bubble response on the rotordynamic forces exerted by the fluid on the turbomachine under cavitating conditions. Inertial, damping, and compressibility effects in the dynamics of the bubbles are included. The effect of the whirl excitation on the two-phase flow is dependent on the wave propagation speed and the bubble resonance behavior in the bubbly mixture. These, in turn, lead to rotordynamic forces which are complicated functions of the whirl frequency and depend on the void fraction of the bubbles and on the mean flow properties. Under cavitating conditions the dynamic response of the bubbles induces major deviations from the non-cavitating flow solutions. The quadratic dependence of rotordynamic fluid forces on the whirl speed, which is typical of cavitation-free operation is significantly modified. Results are presented to illustrate the influence of the various flow parameters.

INTRODUCTION

Rotordynamic instabilities and cavitation represent one of the most severe limitations to the performance of turbopumps (Brennen 1994), especially in high power density applications where they can be responsible for very serious problems, ranging from long term fatigue damage to sudden failure of the machine (Jery *et al.* 1985; Franz *et al.* 1989). The most critical rotordynamic instability in turbopumps is the development of self-sustaining lateral motions (whirl) of the impeller under the action of destabilizing forces. These forces can be of mechanical origin (internal damping and hysteresis of the rotating parts, stiffness anisotropies, dynamic unbalance, direct contact of the static and rotating parts, system nonlinearities, etc.), or of fluid dynamic origin (flow asymmetries, cavitation, journal bearing or seal forces, leakage and recirculation flows, rotor/stator interactions, non-stationary phenomena).

Because of their greater complexity, rotordynamic fluid forces under cavitating conditions have so far received less attention in the open literature, despite their potential for promoting rotordynamic instabilities of high performance turbopumps (Rosenmann, 1965). Recently, forced vibration experiments carried out by Franz (1989) and Bhattacharyya (1994) have demonstrated that cavitation affects the rotordynamic forces on axial flow inducers artificially whirled on a circular orbit with assigned eccentricity and constant whirl speed. The occurrence of cavitation has been found to have, in general, a destabilizing effect on the whirl motion and to reduce the steady lateral forces on the rotor. More importantly in the context of the present work, cavitation alters the behavior of the rotordynamic fluid forces as a function of the whirl speed by replacing the characteristic quadratic dependence typical of cavitation-free operation with a more complex function of frequency. Consequently, the traditional quadratic expansion of the rotordynamic fluid forces in terms of stiffness, damping and inertia matrices seems to be no longer justified for cavitating turbopumps.

The purpose of this research is to obtain some fundamental insight into the fluid dynamic phenomena responsible for the observed behavior of the rotordynamic fluid forces in whirling impellers operating under cavitating conditions. Bhattacharyya (1994) correlated the changes in the rotordynamic fluid forces with the development of reverse (possibly oscillatory) flow in cavitating inducers at lower flow coefficients. This implies some interaction between cavitation, backflow and whirl motion of the inducer, the details of which are not clear.

The purpose of the present study is to investigate the extent to which the behavior of the rotordynamic forces under cavitating conditions could be a consequence of the dynamic response of the bubbly mixture in the blade passages.

This whirling helical flow is studied using the same linear perturbation approach of previous dynamic analyses of bubbly liquids (d'Agostino and Brennen 1983, 1988, 1989; d'Agostino, Brennen and Acosta 1988; Kumar and Brennen 1993). In spite of the intrinsic limitations of the linear approximation and the simplifying assumptions introduced in order to obtain a closed form solution, some of the observed features of the rotordynamic forces are consistent with available experimental results.

LINEARIZED DYNAMICS OF A BUBBLY FLOW IN A WHIRLING IMPELLER

We address the problem of the flow of a bubbly liquid of velocity, $\boldsymbol{u}$, pressure, p, density, ρ, speed of sound, c, void fraction, $\alpha << 1$, in a simple helical inducer rotating with velocity Ω, and whirling on a circular orbit with small eccentricity, ε, at a frequency ω. We define cylindrical coordinates r', ϑ', z', fixed in the impeller and rotating and whirling with it (z' is the impeller axis), and an inertial cylindrical coordinate system, r, ϑ, z, fixed on the axis of the surrounding duct, as illustrated in Figures 1 and 2. A number of simplifying assumptions are introduced in order to obtain a soluble set of equations that still reflect the dynamics of a whirling inducer in a bubbly mixture. The relative motion of the two phases is neglected, as are viscous effects (except in the dynamics of the bubbles where they give important damping contributions). A simple helical inducer with radial blades is considered as shown in Figure 1, with zero blade thickness, hub radius, r_H, tip radius, r_T, axial length, L, small tip blade angle, β_T, constant pitch, $P = 2\pi r_T \tan\beta_T$, axial blading length, L_B, and blade cant angle, $\gamma \cong 0$, in the meridional plane. The suction flow conditions (subscript s) are given by the flow coefficient, ϕ, the uniform axial velocity, $w_s = \phi\Omega r_T$, and the pressure, p_s.

For the present purposes we approximate the mean flow within the inducer as comprising a simple forced vortex with axial velocity

$$w_o = const = \frac{w_s}{1-\alpha}\frac{r_T^2}{r_T^2 - r_H^2}$$

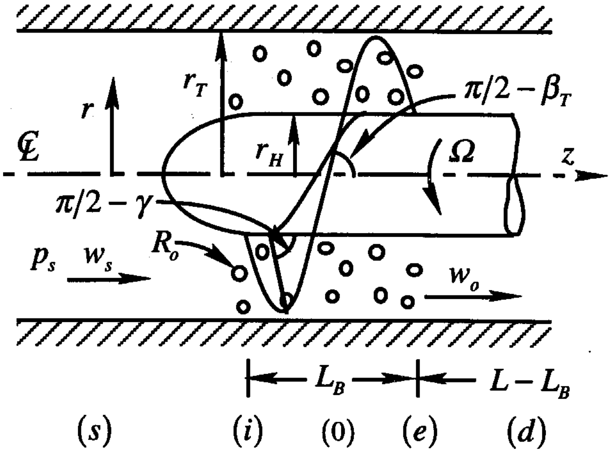

Figure 1. Schematic of the flow and inducer geometry.

The cavitating bubbles are modeled by assuming a homogeneous distribution of small bubbles of unperturbed radius, R_o, with void fraction, $\alpha << 1$. Relative motion between the bubbles and the fluid is neglected.

During its transit through the inducer the bubbly mixture rotationally accelerates from its initial state at the blade inlet to the uniform angular velocity

$$\Omega_o(z) = \frac{v_o}{r} = \Omega\left(1 - \frac{w_o}{\Omega r_T}\cot\beta_{oT}\right)$$

The pressure varies in the inducer with the radius, r, according to the equation:

$$p_o = p_s + \frac{1}{2}\rho\left(w_s^2 - w_o^2\right) + \frac{1}{2}\rho\left[\Omega^2 - (\Omega - \Omega_o)^2\right]r^2$$

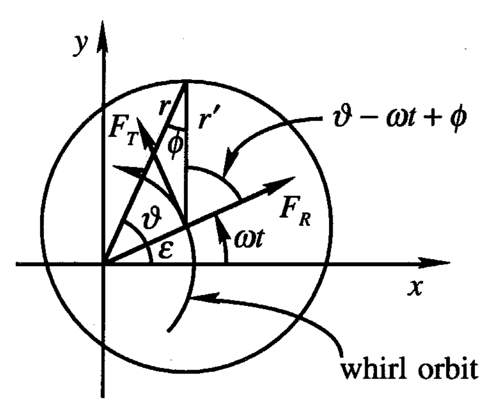

Figure 2. Schematic of whirl motion and rotordynamic forces.

The unperturbed flow inside the inducer is therefore fully specified by the suction conditions, the flow rotation, Ω_o, and the assumed value of the void fraction.

Kinematic conditions of the form $Db/Dt = 0$ are assigned to the flow velocity on the hub ($b = r' - r_H = 0$), on the outer casing ($b = r - r_T = 0$), and on the blade

$$b = \vartheta' - \frac{r'}{r_T}\cot\beta_T \tan\gamma + \frac{z'}{r_T}\cot\beta_T - \vartheta'_B = 0$$

where ϑ'_B identifies the orientation of the blade (Figure 1).

It is convenient to analyze the flow in a Lagrangian frame, r_L, ϑ_L, z_L, moving with the fluid, in which the unperturbed flow is at rest and the perturbation velocity components are indicated by u, v, w. Expressing b in terms of r_L, ϑ_L, z_L and implementing the material derivatives, the linearized boundary conditions are found to be:

$$u = \varepsilon\omega_L \sin(\vartheta_L - \omega_L t) \quad \text{on the hub} \quad r_L = r_H$$

$$u = 0 \quad \text{on the casing} \quad r_L = r_T$$

and, exploiting the fact that in most inducers $\gamma \cong 0$ and $\tan\beta_T << 1$, the blade boundary condition is fully linearized to yield (with error of order $\tan\beta_T$):

$$w = 0 \quad \text{on} \quad z_L \equiv \text{constant}$$

where $\omega_L = \omega - \Omega_o$ is the frequency of the boundary excitation in the Lagrangian frame.

Linearization of the fluid dynamic equations of the bubbly mixture for time-harmonic perturbations of frequency, ω_L, yields the following Helmholtz equation (d'Agostino and Brennen 1988):

$$\nabla^2\hat{p} + k^2(\omega_L)\hat{p} = 0$$

where $\hat{p}$ is the complex amplitude of the pressure fluctuation, such that $\tilde{p} = \hat{p}e^{-i\omega_L t}$ in the inducer flow and the velocity and pressure perturbations are related by $i\omega_L\rho(1-\alpha)\hat{u} = \nabla\hat{p}$. The free-space wave number, k, is determined by the dispersion relation:

$$\frac{1}{c_M^2(\omega_L)} = \frac{k^2(\omega_L)}{\omega_L^2} = \frac{1}{c_{Mo}^2}\left(\frac{\omega_{Bo}^2(1 + i\omega_L R_o/c)}{\omega_B^2 - \omega_L^2 - i\omega_L 2\lambda}\right) + \frac{1-\alpha}{c^2}$$

Here $c_M(\omega_L)$ is the complex and dispersive (frequency dependent) speed of propagation of harmonic disturbances of angular frequency, ω_L, in the free bubbly mixture, and $\omega_B(\omega_L)$ and $\lambda(\omega_L)$ are the effective natural frequency and damping coefficient of an individual bubble when excited at frequency ω_L (Prosperetti 1977, 1984). Also:

$$\omega_{Bo}^2 = \frac{3p_o}{\rho R_o^2} - \frac{2S}{\rho R_o^3} \quad \text{and} \quad c_{Mo}^2 = \frac{\omega_{Bo}^2 R_o^2}{3\alpha(1-\alpha)}$$

where ω_{B0} is the natural frequency of oscillation of a single bubble at isothermal conditions in an unbounded liquid with pressure p_o and surface tension S (Plesset and Prosperetti 1977, Knapp *et al.* 1970) and c_{M0} is the low-frequency sound speed in a free bubbly flow with incompressible liquid ($\omega_L \to 0$ and $c \to \infty$). Notice that the propagation speed and wave number depend on the radial coordinate through the mean pressure p_o, thereby making the Helmholtz equation quasi-linear.

The Helmholtz equation for the pressure, together with the above kinematic conditions and the appropriate inlet and exit conditions, represent, in theory, a quasi-linear boundary value problem for $\hat{p}$. However, further simplifications are necessary in order to obtain a closed form solution. To fully linearize the problem, the wave number k is computed for a reference value $\bar{p}_o$ of the inducer pressure p_o at some suitable mean radius, say $\bar{r}^2 = (r_T^2 + r_H^2)/2$. By separation of variables (Lebedev 1965), the solution for the pressure perturbation, expressed in the absolute coordinates, is readily found to be:

$$p(r,\vartheta,t) - p_o(r) = \mathrm{Im}\left[i\varepsilon r_T \omega_L^2 \rho(1-\alpha) G(r,\omega_L) e^{i(\vartheta - \omega t)}\right]$$

where the function $G(r,\omega_L)$ has the following form:

$$G(r,\omega_L) = \frac{1}{kr_T}\frac{J_1(kr)Y_1'(kr_T) - Y_1(kr)J_1'(kr_T)}{J_1'(kr_H)Y_1'(kr_T) - Y_1'(kr_H)J_1'(kr_T)}$$

with

$$k = k(\omega_L)$$

where J_1, Y_1, J_1', and Y_1' are the normal Bessel functions and their derivatives. Notice that the flow dynamics does not have a simple quadratic dependence on the excitation frequency, except in the incompressible limit where:

$$k \to 0 \quad \text{and} \quad G(r,\omega_L) \to \frac{r/r_T + r_T/r}{1 - r_T^2/r_H^2}$$

so that G is independent of ω_L, as expected.

To evaluate the fluid induced forces per unit length on the inducer and the casing we define:

$$f^{(I)} = -\frac{\int_0^{2\pi}\left[p - p_o + (r - r')\frac{dp_o}{dr}\right]_{r=r_H} e_r' r_H \, d\vartheta}{\pi\varepsilon\rho\Omega^2 r_T^2}$$

$$f^{(C)} = \frac{\int_0^{2\pi} (p - p_o)_{r=r_T} e'_r \, r_T \, d\vartheta}{\pi \varepsilon \rho \Omega^2 r_T^2}$$

where e'_r is the unit vector in the direction of r'. Upon integration, the radial and tangential components of the rotordynamic forces, f_R and f_T, are more compactly represented in complex form by:

$$f^{(I)} = f_R^{(I)} - i f_T^{(I)} =$$

$$= -\left\{ \left[1 - \frac{(\Omega - \Omega_o)^2}{\Omega^2} \right] \frac{r_H^2}{r_T^2} + (1-\alpha) \frac{\omega_L{}^2}{\Omega^2} \frac{r_H}{r_T} G(r_H, \omega_L) \right\}$$

$$f^{(C)} = f_R^{(C)} - i f_T^{(C)} = (1-\alpha) \frac{\omega_L{}^2}{\Omega^2} G(r_T, \omega_L)$$

The entire flow has therefore been determined in terms of the material properties of the two phases, the geometry of the impeller, the nature of the excitation, and the assigned quantities: ϕ, α and R_o / r_T.

RESULTS AND DISCUSSION

The present calculated results for the rotordynamic forces will be compared with the experimental results for a helical inducer obtained by Bhattacharyya (1994). The inducer was operated in water ($\rho = 1000$ kg/m^3, $c = 1485$ m/s, $\mu = 0.001$ Ns/m^2, $S = 0.0728$ N/m) with no prerotation ($\Omega_i = 0$) at $\Omega = 3{,}000$ rpm, and a flow coefficient $\phi = 0.074$. The two-phase flow in the inducer is assumed to contain air bubbles, ($\chi_G = 0.0002$ m^2/s, $\gamma = 1.4$) at mean pressure $\bar{p}_o$, with the void fraction α specified by assigning the parameter $3\alpha(1-\alpha) r_T^2 / R_o^2$.

The propagation of disturbances through the annulus has been examined in detail, because of their central role in determining the rotordynamic fluid forces on the inducer and the casing. Not surprisingly, the general features of linear propagation in the inducer flow are qualitatively similar to those of previous analyses of the dynamics of bubbly flows in other geometric configurations (d'Agostino and Brennen 1983, 1988, 1989; d'Agostino, Brennen and Acosta 1988; Kumar and Brennen 1993). The solution depends on the radial coordinate, r, through a linear combination of first order Bessel functions (properly weighted to satisfy the boundary conditions at the inner and outer radii) and on the excitation frequency, $\omega_L = \omega - \Omega_o$, through the wave number $k = k(\omega_L)$, as illustrated in Figures 3 and 4 for a typical value of the parameter $3\alpha(1-\alpha) r_T^2 / R_o^2 = 100$. Quite similar parameters, also involving the void fraction and the square of the ratio of a macroscopic dimension of the flow to the

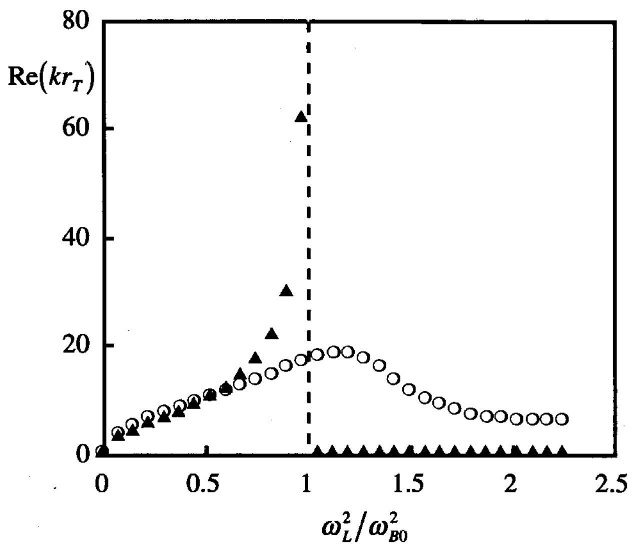

Figure 3. Real part of the normalized radial wave number, kr_T, as a function of the square of the reduced frequency, $\omega_L^2 / \omega_{Bo}^2$, for $3\alpha(1-\alpha) r_T^2 / R_o^2 = 100$, and with (o) and without (▲) damping.

bubble size, appear in all other previous analyses of the dynamics of bubbly flows.

Notice from Figures 3 and 4 that the relative importance of the real and imaginary parts of k is reversed when ω_L / ω_{B0} crosses unity. Consequently, in view of the properties of Bessel functions, appreciable wave-like propagation only occurs at low excitation frequencies, below ω_{B0}, while above ω_{B0} the flow disturbances are rapidly attenuated in the bubbly mixture. Owing to the dependence of ω_{B0} on the bubble size and ambient pressure, this transition is usually unimportant in laboratory experiments on cavitating inducers operating in water at relatively low speed. However, it could be relevant to full-scale high performance turbopumps, where the excitation frequency is higher due to the much larger rotational speeds.

Free oscillations of the flow can only occur if $J_1'(kr_H) Y_1'(kr_T) - Y_1'(kr_H) J_1'(kr_T) = 0$, and we denote the roots of this equation by $k_n r_T = \beta_n$, $n = 1, 2, 3, \ldots$. The roots clearly depend on the hub/tip radius ratio r_H / r_T, and are known to be real, distinct, non-negative, and diverging for large values of n. The first few roots β_n are reported in Table 1 for some representative values of r_H / r_T.

In the absence of damping, the condition for free oscillations, together with the dispersion relation, defines an infinite set of natural frequencies (and mode shapes) for the two-phase flow in the inducer :

$$\omega_n^2 = (\omega - \Omega_o)^2 = \omega_{Bo}^2 \Big/ \left(1 + \frac{3\alpha(1-\alpha) r_T^2 / R_o^2}{\beta_n^2} \right)$$

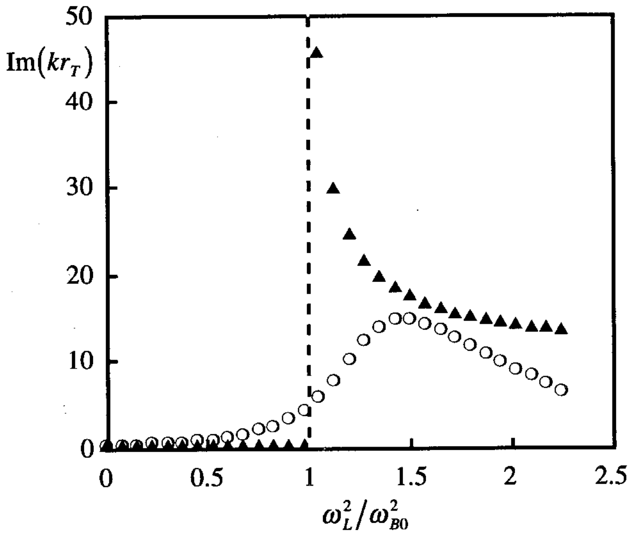

Figure 4. Imaginary part of the normalized radial wave number, kr_T, as a function of the square of the reduced frequency, ω_L^2/ω_{Bo}^2, for $3\alpha(1-\alpha)r_T^2/R_o^2=100$, and with (○) and without (▲) damping.

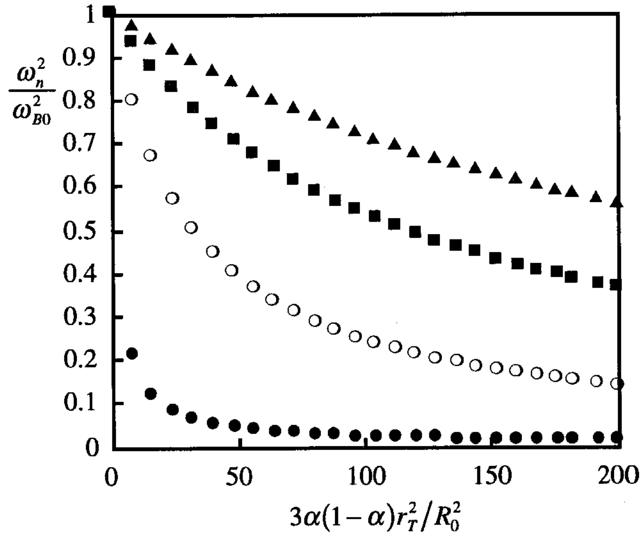

Figure 5. Normalized natural frequency, ω_n^2/ω_{Bo}^2, as a function of the bubble interaction parameter $3\alpha(1-\alpha)r_T^2/R_o^2$ for $n=1$ (●), 2 (○), 3 (■), and 4 (▲) modes.

Hence, the natural frequencies never exceed the bubble resonance frequency, ω_{Bo}, they increase with the mode number, and converge to ω_{Bo} for large values of n. They also decrease with $3\alpha(1-\alpha)r_T^2/R_o^2$, as illustrated in Figure 5 for the lowest modes, and become significantly smaller than ω_{Bo} when $3\alpha(1-\alpha)r_T^2/R_o^2$ is comparable to β_n^2. Also notice from the above equation that the corresponding whirl speeds, ω_n, are shifted by the rotation, Ω_o, of the inducer.

r_H/r_T:	0.3	0.4	0.5	0.6
β_1:	1.582	1.462	1.355	1.262
β_2:	5.137	5.659	6.565	8.041
β_3:	9.308	10.683	12.706	15.801
β_4:	13.684	15.848	18.943	23.6243
β_5:	18.116	21.049	25.205	31.462

Table 1. Zeros of $J_1'(\beta r_H/r_T)Y_1'(\beta)-Y_1'(\beta r_H/r_T)J_1'(\beta)$.

The first few natural mode shapes are shown in Figure 6 as functions of the radial coordinate for $r_H/r_T=0.4$ and $3\alpha(1-\alpha)r_T^2/R_o^2=100$ ($\alpha\cong 0.013$ for the test inducer). These are qualitatively representative of the flow behavior at increasing excitation frequencies, and clearly show that the response of the flow tends to be concentrated in the region close to the hub as the excitation frequency, $\omega_L=\omega-\Omega_o$, approaches ω_{B0}. On the other hand, as mentioned before, when the frequency $\omega_L>\omega_{B0}$, the flow response becomes predominantly of exponential type and is rapidly attenuated with distance from the hub.

The normalized radial rotordynamic force per unit length, $f_R^{(l)}/\pi\varepsilon\rho\Omega^2r_T^2$, for the test inducer is displayed in Figure 7 as a function of the frequency ratio, ω/Ω, for three values of the parameter $3\alpha(1-\alpha)r_T^2/R_o^2$ = 100, 200, and 300. The corresponding rotordynamic force per unit length in the incompressible fluid case is also shown for comparison. Notice that the two-phase flow solution deviates from the quadratic behavior of the incompressible

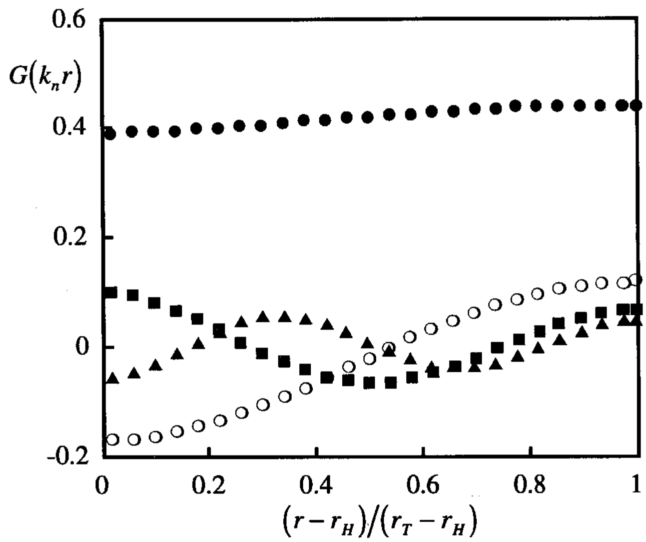

Figure 6. Radial mode shapes, $G(k_nr)$, as functions of $(r-r_H)/(r_T-r_H)$ for several modes $n=1$ (●), 2 (○), 3 (■), and 4 (▲), $r_H/r_T=0.4$, and $3\alpha(1-\alpha)r_T^2/R_o^2=100$.

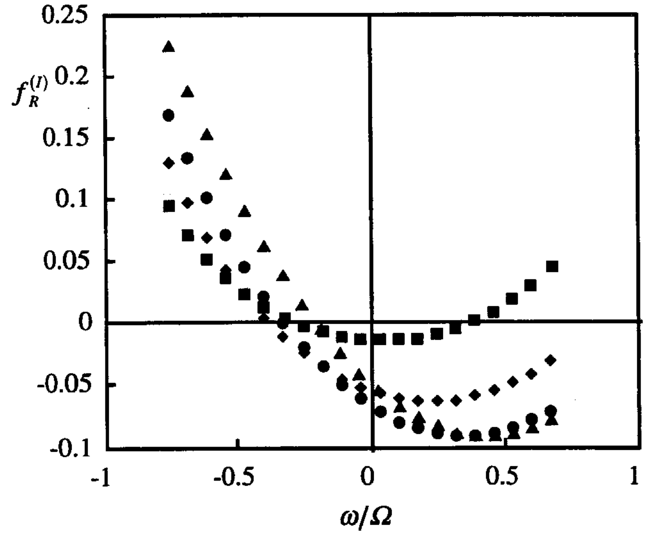

Figure 7. Normalized radial rotordynamic force per unit length, $f_R^{(I)}/\pi\varepsilon\rho\Omega^2 r_T^2$, for the test inducer as a function of the whirl frequency ratio ω/Ω for the incompressible flow case (▲), and in a bubbly fluid with $3\alpha(1-\alpha)r_T^2/R_o^2$ = 100 (●), 200 (◆), and 300 (■). In all cases $\phi = 0.074$, $R_0/r_T = 0.064$.

solution. In particular, for sufficiently high values of $3\alpha(1-\alpha)r_T^2/R_o^2$, the radial rotordynamic force becomes positive at higher values of the whirl frequency ratio.

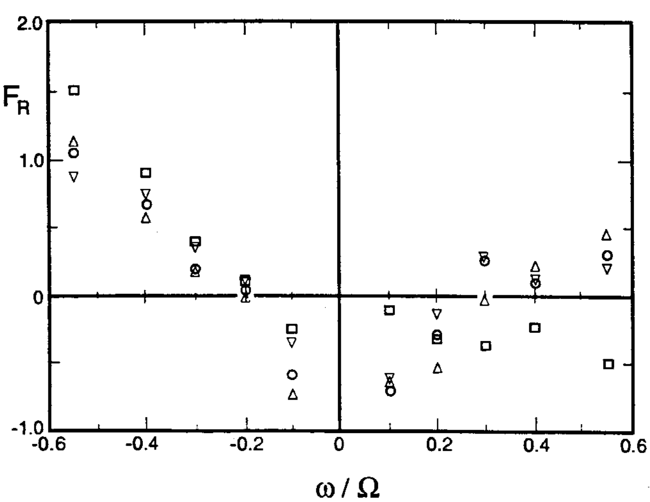

Figure 8. Experimentally measured radial rotordynamic forces for the test inducer as a function of the whirl frequency ratio, ω/Ω, under non-cavitating conditions (□) and with cavitation numbers σ=0.106 (△), 0.098 (○), and 0.093 (▽). In all cases $\phi = 0.074$. (From Bhattacharyya, 1994).

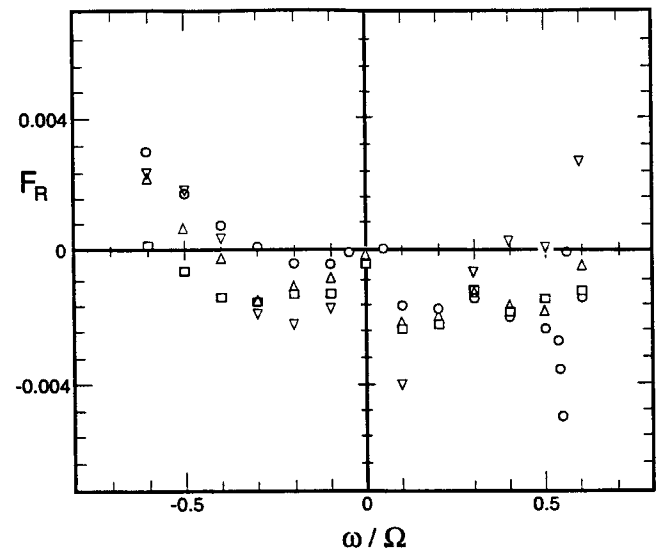

Figure 9. Experimentally measured radial rotordynamic forces on a 12^0 inducer as a function of the nondimensional whirl frequency ratio ω/Ω in the non-cavitating case (○) and with cavitation numbers σ=0.050 (□), 0.040 (△), and 0.035 (▽). In all cases $\phi = 0.070$.

Notice that the calculated behavior is similar to that experimentally observed by Bhattacharyya (1994) and

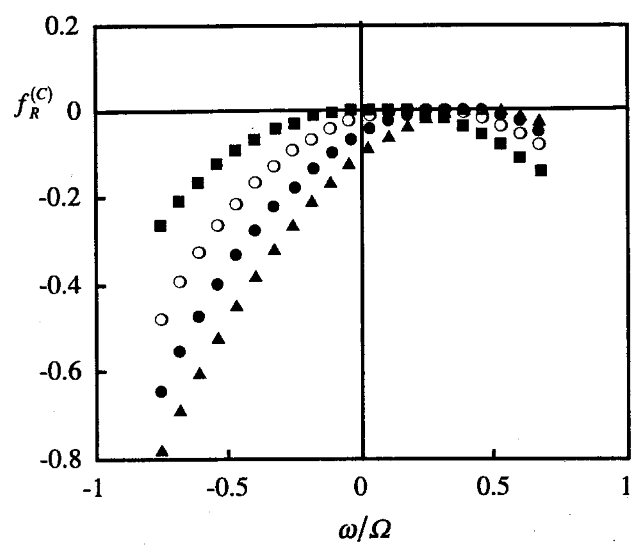

Figure 10. Radial component of the normalized rotordynamic force per unit length, $f_R^{(C)}/\pi\varepsilon\rho\Omega^2 r_T^2$, on the casing as a function of the whirl frequency ratio, ω/Ω, for the incompressible flow case (▲), and in a bubbly fluid with $3\alpha(1-\alpha)r_T^2/R_o^2$ = 100 (●), 200 (○), 300 (■). In all cases $\phi = 0.074$, $R_0/r_T = 0.064$.

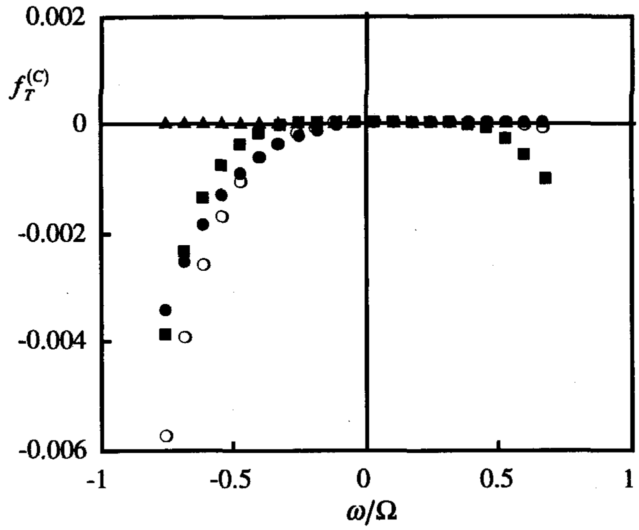

Figure 11. Tangential component of the normalized rotordynamic force per unit length, $f_T^{(I)}/\pi\varepsilon\rho\Omega^2 r_T^2$, on the test inducer as a function of the whirl frequency ratio, ω/Ω, for the incompressible flow case (▲), and in a bubbly fluid with $3\alpha(1-\alpha)r_T^2/R_o^2 = 100$ (●), 200 (○), 300 (■). In all cases $\phi = 0.074$, $R_0/r_T = 0.064$.

similar to those obtained for a 12^0 inducer tested at Caltech (see Figures 8 and 9, for comparison).

Figure 10 presents the normalized radial rotordynamic force per unit length, $f_R^{(C)}/\pi\varepsilon\rho\Omega^2 r_T^2$, on the casing as a function of the whirl frequency ratio, ω/Ω, for the incompressible fluid case and for cavitating conditions given by three values of the parameter $3\alpha(1-\alpha)r_T^2/R_o^2$ = 100, 200, and 300. Again, the presence of cavitation alters the quadratic behavior of the rotordynamic forces.

The present non-viscous model cannot give significant results concerning rotordynamic tangential force. Nevertheless, bubble dynamics effects can be seen even in the framework of the present approximations. In the absence of cavitation, the present inviscid formulation predicts an identically zero tangential force; for cavitating flows with increasing void fraction deviations from the zero value of the tangential force occur as illustrated in Figure 11.

CONCLUSIONS

This study reveals that a number of important effects can occur in the bubbly and cavitating flows in axial flow inducers as a consequence of the strong coupling between the local dynamics of the bubbles and the global behavior of the flow. The propagation of the whirl-induced disturbances within the annulus is significantly modified by the large reduction of the sonic speed in the bubbly mixture. In the presence of the dissipation associated with the dynamics of the bubbles, the spectral response of the flow is essentially dominated by the lowest resonant modes, while the others are effectively damped. Appreciable oscillatory propagation is limited to the frequency range below the bubble resonance condition. At higher frequencies rapidly decaying propagation of the exponential type prevails. The influence of bubble dynamic effects is dependent on the nondimensional parameter $3\alpha(1-\alpha)r_T^2/R_o^2$. The natural frequencies of the flow are always smaller than the bubble resonance frequency and their lowest values decrease rapidly when the bubble interaction parameter $3\alpha(1-\alpha)r_T^2/R_o^2$ exceeds unity. Moreover, the penetration of the whirl-induced disturbances into the flow also decreases with the excitation frequency and the bubble interaction.

As a consequence of these modifications, the rotordynamic fluid forces on the inducer and its casing in bubbly and cavitating flows no longer vary quadratically with the whirl frequency, as in non-cavitating flow. Rotordynamic fluid forces are also influenced by the flow rotation in the inducer, which changes the frequency of the excitation seen by the bubbly mixture. The spectral response of the rotordynamic fluid forces is strongly correlated to the bubble interaction parameter and the relative magnitude of the excitation and bubble resonance frequencies. Given the void fraction and bubble size typical of cavitating inducers, the resonant transition is usually unimportant in low-speed laboratory experiments, but may play an important role in full-scale turbopumps operating at much higher speeds.

The present theory invoked major simplifications and approximations and therefore is not expected to provide a quantitative description of unsteady bubbly and cavitating flows in whirling inducers. In this respect, the most crucial limitation is probably the relatively crude description of the unperturbed flow through the inducer. The linearization of the bubble dynamic response is more justified because of the expected magnitudes of the bubble size and rotor eccentricity in whirling turbopumps. Another limitation of the theory consists of the need to assign the value of the bubble interaction parameter, rather than deduce it from the mean flow conditions by means of a suitable cavitation model. However, experimental information on the typical void fraction and bubble size in cavitating inducers is more readily obtained than direct measurements of the fluid forces. Despite these limitations, the present analysis is qualitatively consistent with experimental results and reveals some of the fundamental phenomena that play a crucial role in determining the rotordynamic fluid forces in cavitating inducers.

ACKNOWLEDGMENTS

This work has been supported by the Italian Department of Universities and Scientific & Technologic

Research under the 1993 grant program for academic research and by the Office of Naval Research under grant number N-00014-91-K-1295. Some of the authors would like to express their gratitude to Profs. Mariano Andrenucci and Renzo Lazzeretti of the Aerospace Engineering Department of Pisa University, Pisa, Italy, for their encouragement in the completion of the present work.

REFERENCES

Bhattacharyya, A., 1994, "Internal Flows and Force Matrices in Axial Flow Inducers", *Ph.D. Thesis*, Division of Engineering and Applied Science, California Institute of Technology, Pasadena California.

Brennen, C. E., 1994, "Hydrodynamics of Pumps", Concepts ETI, Inc. and Oxford University Press.

Ceccio, S.L., and Brennen, C.E., 1990, "Observations of the Dynamics and Acoustics of Attached Cavities", *ASME Cavitation and Multiphase Flow Forum*, Toronto, Ontario, Canada, pp. 79-84.

d'Agostino, L., and Brennen, C.E., 1983, "On the Acoustical Dynamics of Bubble Clouds", *ASME Cavitation and Multiphase Flow Forum*, Houston, Texas.

d'Agostino, L., and Brennen, C.E., 1988, "Acoustical Absorption and Scattering Cross-Sections of Spherical Bubble Clouds", *J. Acoust. Soc. Am.*, No. 84 (6), pp. 2126-2134.

d'Agostino, L., and Brennen, C.E., 1989, "Linearized Dynamics of Spherical Bubble Clouds", *J. Fluid Mech.*, Vol. 199, pp. 155-176.

d'Agostino, L., Brennen, C.E., and Acosta, A.J., 1988, "Linearized Dynamics of Two-Dimensional Bubbly and Cavitating Flows over Slender Surfaces", *J. Fluid Mech.*, Vol. 192, pp. 485-509.

Franz, R., 1989, "Experimental Investigation of the Effect of Cavitation on the Rotordynamic Forces on a Whirling Centrifugal Pump Impeller", *Ph. D. Thesis*, Division of Engineering and Applied Sciences, California Institute of Technology, Pasadena, California.

Franz, R., Acosta, A.J., Brennen, C.E., and Caughey, T.K., 1989, "The Rotordynamic Forces on a Centrifugal Pump Impeller in the Presence of Cavitation", *Proc. ASME Symp. Pumping Machinery – 1989* (ed. P. Cooper), FED-Vol. 81, pp. 205-212.

Greitzer, E.M., 1980, "The Stability of Pumping Systems", *ASME J. Fluids Eng.*, Vol. 103, pp. 193-242.

Jery, B., 1987, "Experimental Study of Unsteady Hydrodynamic Force Matrices on Whirling Centrifugal Pump Impellers", *Report No. E200.22*, Division of Engineering and Applied Sciences, California Institute of Technology, Pasadena, California.

Jery, B., Brennen, C.E., Caughey, T.K., and Acosta, A.J., 1985, "Forces on Centrifugal Pump Impellers", *2nd Int. Pump Symp.*, Houston, Texas, April 29-May 2, 1985.

Knapp, R. T., Daily, J. W., and Hammit, F. G., 1970, "Cavitation", *McGraw Hill.*

Kumar, S., and Brennen, C.E., 1993, "Some Nonlinear Interactive Effects in Bubbly Clouds", *J. Fluid Mech.*, Vol. 253, pp. 565-591.

Lakshminarayana, B., 1982, "Fluid Dynamics of Inducers – A Review", *ASME J. Fluids Eng.*, Vol. 104, pp. 411-427.

Lebedev, N.N., 1965, "Special Functions and Their Applications", *Prentice Hall.*

Plesset, M. S., and Prosperetti, A., 1977, "Bubble Dynamics and Cavitation", *Ann. Rev. Fluid. Mech.*, Vol. 9, pp. 145-185.

Prosperetti, A., 1977, "Thermal Effects and Damping Mechanisms in the Forced Radial Oscillations of Gas Bubbles in Liquids", *J. Acoust. Soc. Am.*, Vol. 61, No. 1 (6), pp. 17-27.

Prosperetti, A., 1984, "Bubble Phenomena in Sound Fields: Part One", *Ultrasonics*, March 1984, pp. 69-78.

Rosenmann, W., 1965, " Experimental Investigations of Hydrodynamically Induced Shaft Forces with a Three Bladed Inducer", *Proc. ASME Symp. on Cavitation in Fluid Machinery*, pp. 172-195.

Shepherd, D.G., 1956, "Principles of Turbomachinery", *The Macmillan Company*